RUNNING TITLE: Mercury, dissolved organic matter, and microbiomes

Linkages among *Clostridia*, recalcitrant organic matter, and methylmercury production in oligotrophic sediments

Emily B. Graham[1*], Joseph E. Knelman[2], Rachel S. Gabor[3], Shon Schooler[4], Diane M. McKnight[5,6,7], Diana R. Nemergut[5,8]

[1]Biological Sciences Division, Pacific Northwest National Laboratory, Richland, WA, USA

[2]Joint Genome Institute, US Department of Energy, Walnut Creek, CA, USA

[3]Department of Geology and Geophysics, University of Utah, Salt Lake City, UT, USA

[4]Lake Superior National Estuarine Research Reserve, University of Wisconsin-Superior, Superior, WI, USA

[5]Institute for Arctic and Alpine Research, University of Colorado at Boulder, Boulder, CO, USA

[6]Civil Engineering Department, University of Colorado at Boulder, Boulder, CO, USA

[7]Environmental Studies Program, University of Colorado at Boulder, Boulder, CO, USA

[8]Biology Department, Duke University, Durham, NC, USA

The authors declare no conflict of interest.

Correspondence: Emily B. Graham, emily.graham@colorado.edu; Biological Sciences Division; Pacific Northwest National Laboratory; 902 Battelle Blvd.; Richland, WA, 99354; (509) 372-6049

Abstract.

Recent advances have allowed for greater investigation into microbial regulation of mercury toxicity in the environment. In wetlands in particular, dissolved organic matter (DOM) may influence methylmercury (MeHg) production both through chemical interactions and through substrate effects on microbiomes. We conducted microcosm experiments in two disparate wetland environments (unvegetated and vegetated sediments) to examine the impacts of plant leachate and inorganic mercury loadings on microbiomes, DOM cycling, and MeHg production. We show that while leachate influenced the microbiome in both environment types, sediment with high organic carbon content was more resistant to change than oligotrophic sediment. Oligotrophic unvegetated sediments receiving leachate produced more MeHg than unamended microcosms, coincident with an increase in putative chemoorganotrophic methylators belonging to *Clostridia*. Further, metagenomic shifts toward fermentation, and secondarily iron metabolisms, in these microcosms as well as degradation of complex DOM also support a possible association between rarely acknowledged microorganisms and MeHg. Our research provides a basis for future investigation into the role of fermenting organisms in mercury toxicity and generates a new hypothesis that DOM can stimulate mercury methylation either 1) via direct methylation by fermenting bacteria or 2) via enhancing carbon bioavailability for sulfate- and iron-reducing bacteria through breakdown of complex DOM.

Introduction.

Mercury methylation in anoxic sediments is central to the bioaccumulation of mercury in plant and animal tissue[1-3] and poses a significant environmental and human health concern in freshwater wetlands[4-6]. Dissolved organic matter (DOM) has been a focus of geochemical investigations for decades, and both positive and negative interactions between DOM and mercury methylation – principally, a microbial transformation[7] – have been demonstrated under contrasting environmental conditions[7-9]. While the microbial mechanisms generating methylmercury are poorly understood, the recent discovery of the *hgcAB* gene cluster has allowed investigations into the microbial ecology of mercury cycling[10-13]. In particular, interactions between environmental microbiomes, DOM quantity and quality, and mercury methylation in natural systems remain an uncertainty in predicting hotspots of mercury toxicity in the environment[7,14].

Dissolved organic matter is comprised of various classes of organic compounds (primarily organic acids) with a wide range of molecular weights and aromaticities[15,16]. DOM concentrations are elevated in wetlands relative to other freshwater systems (>10 mg/L), and the humic fraction derived from plant leachate predominates. With respect to mercury cycling in wetlands, mercury methylation is impacted both by binding properties of the humic DOM fraction, resulting either in increased dissolution of inorganic mercury complexes or in physical inhibition of mercury bioavailability[17-19], and by provisioning organic substrate for microbial activity[7,15,20]. These effects may also vary with ambient geochemistry, as Graham *et al.*[9] have demonstrated that sulfide concentrations and DOM aromaticity interact to influence MeHg production. Further, interactive effects of sediment microbiomes and DOM biogeochemistry are less well-resolved than other aspects of linkages between environmental geochemistry and

mercury toxicity. Numerous studies have shown regulation of freshwater microbial communities by DOM quantity or quality[21-23], and such changes in environmental microbiomes may alter ecosystem biogeochemical cycling[24]. The character of humic DOM (putatively most influential to mercury methylation) can be assessed at scales relevant to microbial activity with fluorescence spectroscopy, which correlates changes in humic fluorescence relative to other portions of the optically-active DOM pool[25].

Recent work has increased knowledge on the microbiology of mercury methylation, expanding potential microorganisms mediating methylation beyond sulfate-reducing bacteria[7,26], iron-reducing bacteria[27] and methanogens[28]. To date, all tested microorganisms containing the *hgcAB* gene cluster have been confirmed as methylators, and the gene appears to be highly conserved allowing it to serve as a genetic marker for methylating organisms[7,12]. Gilmour *et al.*[12] have identified five clades of putative methylators, including new clades of syntrophic and *Clostridial* organisms. While research has provided insight into the abundance of these new organisms in mercury-contaminated landscapes[29-31], many studies have continued to focus on the involvement of sulfate-[32,33] and iron-reducing bacteria[34] as well as methanogens[35] in mercury methylation. As such, the importance of organisms with alternative metabolisms in mercury methylation remain relatively unexplored. Resolving interactions between sediment microbiomes, environmental chemistry, and inorganic mercury complexes is thought to be central in understanding variation in methylation rates among natural systems[7,12,36].

Here, we examine the influence of DOM from plant leachate on net methylmercury (MeHg) production in a contaminated freshwater estuary at the base of Lake Superior. We hypothesize that environmental biogeochemistry (in particular, DOM quantity and quality) influences mercury methylation both by regulating microbial activity and by shifting the

abundance and metabolic diversity of mercury methylators. We test this hypothesis across chemically distinct sediments associated with unvegetated (oligotrophic) and vegetated (high-C) environments, using a microcosm experiment to monitor changes in sediment microbiomes, DOM chemical quality, and net MeHg production in response to additions of leachate from overlying plant material. Our results provide evidence for the involvement of metabolisms that ferment recalcitrant organic matter in mercury methylation, particularly within oligotrophic unvegetated environments, an effect that may be imperative to understanding and mitigating human exposure to MeHg with increasing DOM deposition into aquatic environments[37].

Methods.

Field site.

The St. Louis River Estuary is home to the largest U.S. port on the Great Lakes and covers roughly 12,000 acres of wetland habitat directly emptying into Lake Superior. Mining in the headwaters, industrial discharge in the port, and atmospheric deposition have left a legacy of mercury contamination in the sediment. We obtained sediment samples from vegetated (*Zizania palustris* (wild rice), 46^{o} 40.855' N, 91^{o} 59.048'W) and unvegetated (46^{o} 41.918' N, 92^{o} 0.123' W) patches in Allouez Bay and wild rice plant matter from nearby Pokegama Bay (46.683448^{o}N, 92.159261^{o}W) to minimize sampling impacts. Both habitats are clay influenced embayments that drain an alluvial clay plain created by deposition during the retreat of the last glaciation approximately 10,000 years BP.

Experimental design.

A total of 20 anoxic microcosms were constructed in September 2013 to investigate relationships between sediment microbiomes, DOM chemical quality, and mercury methylation. Sediment was obtained in 250-mL amber Nalgene bottles from the top 10 cm of sediment using a block sampling design described in the Supplemental Material. Leachate was extracted using 1 g dried, ground plant matter:20 mL of Nanopure water, filtered through Whatman 0.7 μm GFF filters (Whatman Incorporated, Florham Park, NJ, USA). Microcosms were constructed in 500-mL airtight glass mason jars and stored at room temperature in the dark in Mylar bags with oxygen-absorbing packets between subsampling. Our experiment was designed to promote microbial MeHg production by minimizing abiotic photo-methylation and -demethylation[3] and sustaining a low redox environment to inhibit demethylation[38]. All experimental set up and sample processing was conducted in an anaerobic glovebox containing 85% N_2, 5% CO_2, and 10% H_2 gas mix at the USGS in Boulder, CO. Jars were degassed in the glovebox for 48hr prior to experimentation to remove oxygen.

A full-factorial design was employed with two environments (vegetated and unvegetated sediment) and two treatments (plant leachate and Nanopure water). Sediments were homogenized via mixing but unsieved to maintain environment characteristics. Large roots (>1 cm) were infrequent and removed to lessen heterogeneity among replicates. Each microcosm received 100 g wet sediment, and 250 mL solution consisting either of leachate at 100 mg/L (~5x natural concentrations to mimic a loading event) and $HgCl_2$ at 20 mg/L (50 μg/g wet sediment) in Nanopure water (leachate replicates) or solely of $HgCl_2$ at 20 mg/L in nanopure water (no leachate replicates). The purpose of $HgCl_2$ addition at high concentration was to negate initial differences in mercury, overcome $HgCl_2$ inaccessibility due to abiotic organo-metal interactions, and provide substrate for the duration of the experiment. $HgCl_2$ concentrations were comparable

to microcosm experiments of similar design[39-42], and we estimate minimal dosage effects as communities without leachate did not change through time in unvegetated microcosms and only slightly changed through time in vegetated microcosms (R^2 = 0.19, see results and Fig S1). Microcosms were incubated for 28 days, and subsamples of sediment and water were taken every seven days for analysis of sediment microbiomes and DOM characteristics.

Sediment chemistry, extracellular enzyme activity, and mercury methylation.

Percent carbon and nitrogen, NO_3^-/NO_2^-, NH_4^+, total particulate organic carbon (TPOC), total dissolved nitrogen (TDN), pH, and extracellular enzyme activities of β-1,4-glucosidase, β -1,4-N-acetylglucosaminidase, and acid phosphatase were determined on pre-incubation sediments, as described in the Supplemental Material. For total- and methylmercury analysis, initial (day 0) and final (day 28) subsamples were frozen at -70^{o}C, freeze-dried, and sent on dry ice to the USGS Mercury Lab in Middleton, WI for analysis by aqueous phase ethylation, followed by gas chromatographic separation with cold vapor atomic fluorescence detection (Method 5A-8), acid digestion (Method 5A-7), and QA/QC. Mercury analyses were performed on 3 of 5 replicates for each environment and microcosm type. All other analyses were performed on 5 replicates, except for no unvegetated microcosms without leachate beyond day 0 (n = 4, one replicate destroyed during experiment).

Dissolved organic matter characteristics.

Water subsamples were collected at 7-day intervals (days 0, 7, 14, 21, and 28) to determine non-purgeable organic carbon (NPOC) concentration and specific UV absorbance at 254 nm ($SUVA_{254}$) as well characteristics of the optically active DOM pool (mostly associated

with humic DOM fraction), as described in the Supplemental Material. We calculated the fluorescence index (FI) to determine the relative contribution of microbial vs. terrestrial matter to the DOM pool, the humic index (HIX) to identify large aromatic compounds consistent with humic material, and the freshness index to determine the availability of labile carbon[25,43] using MATLAB software (2013a, The MathWorks, Natick, MA) according to Gabor *et al.*[44].

Microbial DNA extraction, 16S rRNA amplicon, and metagenomic shotgun sequencing.

DNA from each sediment subsample was extracted using the MO Bio Power Soil DNA Extraction kit (MO BIO Laboratories, Carlsbad, CA, USA), as described in Knelman *et al.*[45]. The region encoding the V4 fragment of the 16S rRNA gene was amplified with the primers 515F/806R, using the PCR protocol described by the Earth Microbiome Project[46] (Supplemental Material). The final multiplexed DNA samples were sequenced at CU-Boulder (BioFrontiers Institute, Boulder, CO) on an Illumina MiSeq with the MiSeq Reagent Kit v2, 300 cycles (Illumina, Cat. # MS-102-2002) to generate 2 x 150-bp paired-end reads. Sequences are available at XXXXXX. In addition, 3 unvegetated leachate replicates at day 0 (before leachate addition) and day 28 were sent to the Joint Genome Institute (JGI) for shotgun metagenomic sequencing on the Illumina HiSeq platform. Sequences are available at XXXXX.

Sequence analysis.

Partial 16S rRNA gene were filtered for sequence length and minimum quality score in the UPARSE pipeline[47] and OTUs were assigned using QIIME[48] (Supplemental Material). Metagenomic shotgun sequences were assembled and classified against the protein families

database (Pfam)[49], Clusters of Orthologous Groups of proteins (COG)[50], and Kyoto Encyclopedia of Genes and Genomes (KEGG)[51] by JGI via the IMG database pipeline[52].

In addition, 46 of 52 genomes identified by Parks *et al.*[10] were represented by complete or partial 16S rRNA gene sequences in the NCBI GenBank database[53], spanning all clades of methylators. We used two different approaches to determine methylator relative abundance and community structure. To determine relative abundance, we combined available methylating sequences with generated sequences and re-preformed *de novo* OTU-picking. We then identified OTUs containing known methylator sequences as potential methylators. Because of high *Deltaproteobacteria* abundance, many closely-related methylator sequences may have clustered with non-methylating *Deltaproteobacteria* in this approach. Thus, to examine methylator community structure at finer resolution, we created a database of known methylator sequences and performed closed-reference OTU-picking in QIIME against this database. In addition, a BLAST database was constructed from all *hgcA* and *hgcB* gene sequences available in GenBank. A BLASTX search was conducted against this database to identify taxonomic affiliation of methylators in our samples; however, our query resulted in no matches, likely due to inadequate sequencing depth.

Statistical analysis.

All analyses, unless otherwise noted, were conducted using the *R* software platform. Shapiro-Wilk tests were used to verify normality and assess the appropriateness of parametric vs. non-parametric tests. Multivariate sediment properties (*e.g.*, sediment geochemistry, extracellular enzyme activity, and DNA quantity) were compared across environments at day 0 with Hotelling's T-square Test and post hoc Student's *t*-tests. MeHg production was calculated by

178 subtracting day 0 from day 28 MeHg concentrations; values below detection limit were assigned
179 the detection limit as a value for a conservative estimate of change. MeHg production was
180 compared across groups using ANOVA. Changes in DOM indices (FI, freshness, HIX) through
181 time (days 0, 7, 14, 21, and 28) in each sample group were assessed with linear and quadratic
182 regressions. DOM samples with $SUVA_{254}$ >7 were removed due to fluorescence interference
183 from inorganic molecules. Comparisons of DOM indices between data subsets were conducted
184 with ANOVA and post hoc Tukey HSD.

185 Microbial community dissimilarity matrices based on 16S rRNA sequences were
186 constructed using the weighted UniFrac method[54] in QIIME. We preformed analysis using the
187 full community and within the methylating community. To examine the relative abundance of
188 our methylating OTUs, we removed OTUs with less than eight total occurrences (bottom
189 quartile) in our 91 subsamples to limit artifacts from sequencing errors among rare organisms
190 (methylating OTUs were <1% of sequences). Alpha diversity for each sample was assessed using
191 the PD whole tree metric in QIIME. The relative abundance of methylators was compared within
192 each environment at days 0 and 28 (leachate vs. no leachate) using unpaired one-way Student's *t*-
193 tests.

194 Changes in community structure through time (days 0, 7, 14, 21, 28) were assessed with
195 ANOSIM in QIIME. Differences in alpha diversity at day 0 were assessed using unpaired one-
196 way Student's *t*-tests. Relative abundances of major clades were assessed between vegetated and
197 unvegetated environments at day 0 and changes in clades through time (days 0, 7, 14, 21, 28)
198 were assessed using non-parametric Kruskal-Wallis tests with FDR-correct *P* values. SIMPER
199 analysis was conducted using the 'vegan package' to identify OTUs associated with community
200 dissimilarity between days 0 and 28 in microcosms receiving leachate. Correlations between

methylating clades that exhibited significant changes (Kruskal-Wallis, days 0, 7, 14, 21, 28), HIX, and MeHg production were assessed at day 28 using the Pearson product-momentum correlation coefficient, grouping leachate and no leachate microcosms within each environment in a single analysis to provide sufficient variation.

Increases in the frequency of COGs, Pfams, and KEGG pathways at day 28 relative to day 0 were evaluated using binomial tests. Targets more abundant at day 28 (FDR-corrected $P < 0.01$) were examined for correlations with HIX and MeHg production at day 28 with the Pearson product-momentum correlation coefficient.

Results.

Ambient geochemistry and microbiology.

Physicochemical and biological properties of vegetated and unvegetated environments significantly differed (Hotelling $P = 0.004$, Table 1). The unvegetated environment was extremely oligotrophic, with low concentrations of sediment C and N, and both vegetated and unvegetated environments appeared to be N-limited (C:N 16.43 and 20.06). DNA concentration, enzyme activities, and mercury concentrations were an order of magnitude higher within the vegetated environment (Table 1).

Microbial community structure and alpha diversity were significantly different between the two environments (ANOSIM, $P = 0.001$, R= 1.00, *t*-test, P = 0.01), though major phyla were similar (Table 1) and both environments were bacteria (vs. archaea) dominated. The relative abundance of methylators was higher in the vegetated environment (*t*-test, $P = 0.005$), and the structure of potential methylators within microbial communities also differed between environments (ANOSIM, $P = 0.001$, R = 0.99).

Microbiome response to $HgCl_2$ and leachate addition.

Over the course of the incubation, microcosms with vegetated, high-C sediment produced over ten times more MeHg than unvegetated sediment microcosms, regardless of leachate amendment (ANOVA $P = 0.002$, Figure 1). Mercury methylation was enhanced by leachate within the unvegetated nutrient-poor environment with roughly two to four times more production in microcosms receiving leachate as compared to those without leachate. However, leachate did not stimulate MeHg production in the vegetated environment.

Community structure changed through time in vegetated and unvegetated environments with leachate (ANOSIM across days 0, 7, 14, 21, 28, veg.: $P = 0.001$ R = 0.40, unveg.: $P = 0.001$ R = 0.43, Figure S1A and B), but not without leachate (veg.: $P = 0.02$, R = 0.19, unveg.: $P > 0.05$, Figure S1A and B), indicating no substantial effect from high concentrations of added mercury. At day 28, communities in unvegetated microcosms with leachate were different than those without leachate (ANOSIM, $P = 0.01$, R = 0.54), while structure in vegetated sediment microcosms only weakly differed between leachate and no leachate groups ($P = 0.04$, R = 0.22). When examining only potential methylators, the relative abundance of methylators was significantly greater in lechate microcosms versus no leachate for each environment at day 28 (Figure 2A, *t*-test, veg.: $P = 0.04$, unveg.: $P = 0.04$). However, for both environments, there were no significant changes in community structure within methylating clades through time (ANOSIM across days 0, 7, 14, 21, 28, $P > 0.05$). This result was not unexpected given our small sample sizes (methylator OTUs contained less than 1% of sequences).

Changes in community structure in response to leachate was partially generated by an increase in *Clostridia* in both environments (Kruskal-Wallis, veg.: FDR-corrected $P = 0.003$,

unveg.: P = 0.018, Figure 2B, Table S3) and a decrease in *Deltaproteobacteria* in unvegetated sediment (Kruskal-Wallis, veg.: FDR-corrected P = 0.36, unveg.: FDR-corrected P = 0.015, Figure 2B). In particular, *Clostridia* abundances increased by 3-fold (1.1% to 3.8% of the microbiome) and 10-fold (1.5% to 10.5% of the microbiome), respectively in vegetated and unvegetated environments, driven by increases in nearly all families of *Clostridia*. These shifts were mirrored within our subset of data containing only suspected methylators (Figure 2C), which showed distinct (non-significant) trends for increases in *Clostridia* and decreases in *Deltaproteobacteria* in response to leachate in both environments.

Changes in the methylating community were more evident at finer taxonomic levels. One family of *Clostridia* (*Peptococcaceae*), sharply increased with leachate in unvegetated sediment and displayed a similar trend in vegetated sediment (Kruskal-Wallis, veg.: FDR-corrected P = 0.18, unveg.: FDR-corrected P = 0.04, Figure 2D). These changes were due to increases in two closely related methylating OTUs (Kruskal-Wallis, *Dehalobacter restrictus* veg.: FDR-corrected P = 0.24 (uncorrected P = 0.04), and *Syntrophobotulus glycolicus*, unveg.: FDR-corrected P = 0.006) grouped in a single genus by our classification system (*Dehalobacter_Syntrophobotulus*, Kruskal-Wallis, veg.: FDR-corrected P = 0.09, unveg.: FDR-corrected P = 0.0027, Figure S2). Increases in *Clostridia* (*t*-test, FDR-corrected P = 0.006), *Peptococcaceae* (*t*-test, FDR-corrected P = 0.018), *Dehalobacter restrictus* (*t*-test, FDR-corrected P = 0.024), and *Syntrophobotulus glycolicus* (*t*-test, FDR-corrected P = 0.042) as well as a possible trend for decreases in *Deltaproteobacteria* (*t*-test, FDR-corrected P = 0.18) were also reflected in metagenomic data (Figure 3D).

SIMPER analysis of 16S rRNA genes associated with methylator taxonomy in unvegetated leachate microcosms indicated that two OTUs, in *D. restrictus* (increase) and in

Geobacter (decrease), significantly contributed to community differences between day 0 and day 28 ($P < 0.05$, Table S1). This was reflective of broader changes in the full community, in which 22.9% of 175 SIMPER-identified OTUs belonged to *Clostridia* (increased from avg. 0.78 OTUs/sample to avg. 17.20 OTUs/sample, Table S3) while 8% belonged to *Deltaproteobacteria* (decreased from avg. 8.5 OTUs/sample to 7.4 OTUs/sample, Table S2).

In total, 7,150 KEGG pathways, 84 COGs, and 79 Pfams were significantly more abundant at day 28 relative to day 0 in unvegetated leachate microcosms (Figure 3A-C). All classfication systems revealed metabolic shifts towards glycosyltranseferases, among other pathways involved in DOM oxidation and in iron and nitrate reduction.

Changes in DOM chemistry.

Details of DOM quantity and quality changes are presented in the Supplemental Material (Figure S3) and regression statistics are presented in Table 2.

DOM fluorescence indices displayed notable changes through time. In the vegetated environment, FI remained stable at a low value in leachate microcosms, indicating plant-derived DOM, and rose in microcosms without leachate indicating greater relative contribution of microbial vs. abiotic processing (Figure 4A and B). In contrast, in the vegetated environment, HIX increased in both leachate and no leachate microcosms indicating processing of more labile vs. recalcitrant DOM (Figure 4C and D). This increase in HIX corresponded with decrease in freshness (Figure 4E and F), further supporting our interpretation. In the unvegetated environment, leachate microcosms (but not microcosms without leachate) increased in FI (Figure 4A and B) denoting progressively microbial DOM sources. There was no change in HIX (Figure

4C and D) suggesting equal processing of labile vs. recalcitrant DOM. Freshness varied non-linearly in leachate microcosms but not those without leachate (Figure 4E and F).

Across environment types, HIX was significantly higher in vegetated microcosms (ANOVA $P < 0.0001$, Tukey HSD, leachate: $P < 0.0001$, no leachate: $P = 0.004$). FI and freshness were higher in unvegetated leachate microcosms than in vegetated DOM-amended microcosms (Tukey HSD, FI: $P = 0.003$, freshness: $P = 0.03$) but did not differ across microcosms without leachate (Tukey HSD, FI: $P = 0.89$, freshness: $P = 0.40$).

Correlation of microbiome, DOM characteristics, and MeHg production.

Given the apparent shift in community structure towards *Clostridia*, and (chemoorganotrophic) *Peptococcaceae* in particular, we examined correlations of this family with the proportion of complex organic matter (HIX) and MeHg production within each environment. We focused on HIX because this index changed consistently and reflected portions of recalcitrant carbon substrate pools utilized by the organisms we identified. Because we only calculated net MeHg production at the conclusion of the incubation, we analyzed these correlations at day 28 and grouped leachate and no leachate replicates within each environment to provide sufficient variation and sample size. *Peptococcaceae* was negatively correlated with HIX and positively correlated with MeHg production in unvegetated microcosms (Pearson's r ($n = 6$), HIX: $P = 0.001$, $r = -0.96$, MeHg: $P = 0.03$, $r = 0.81$). *Peptococcaceae* abundance in vegetated microcosms did not correlate with HIX ($P = 0.20$) or MeHg production ($P = 0.45$).

Finally, despite low statistical power ($n = 3$), we observed marginally significant trends ($P < 0.10$) between key metabolic pathways and HIX (Table 3). In particular, COGs classified

as: Glycosyltransferase, Glycosyltransferases involved in cell wall biogenesis, Glycosyltransferases - probably involved in cell wall biogenesis, and Beta-galactosidase/beta-glucuronidase; and Pfams classified as: Glycosyl transferase family 2, Radical SAM superfamily, and SusD family displayed significant correlations with HIX at the $P < 0.10$ level. Only Pfam PF00593, TonB dependent receptor, correlated with MeHg production ($P < 0.001$, $r = -1.00$, Table 2).

Discussion.

Mercury methylation across environments.

Geochemical and microbial characteristics varied across environments, resulting in differential patterns of net MeHg production. Within the high-C vegetated environment, leachate did not influence the sediment microbiome or net MeHg production to the same extent as within the more oligotrophic unvegetated environment (Figure 1, Figure S1). Given high ratios of C:N, high OC content, and low NO_3^- concentrations in our vegetated sediment (Table 1), N-limitation may have mitigated net MeHg production in vegetated environments relative to the unvegetated environment[55], which had substantially lower concentrations of all measured C and nutrient concentrations. Both ambient MeHg levels and net MeHg production were an order of magnitude higher in the vegetated environment, supporting other findings that plant-microbe interactions facilitate MeHg production[56-58]. Indeed, the vegetated environment displayed higher ambient DNA concentration, enzyme activities, and methylator abundance, underlying a higher *in situ* rate of biological activity.

By contrast, the unvegetated environment experienced a dramatic increase in MeHg (Figure 1) in response to leachate that correlated with changes in the sediment microbiome (Figure 2 and 3, Figure S1). Carbon limitation has been widely demonstrated as a constraint on

338 microbial activity[59-61]; thus, leachate may bolster MeHg production in C-limited ecosystems via
339 impacts on microbial activity. In our system, net MeHg production in the unvegetated
340 environment was possibly also constrained by low *in situ* rates of microbial activity and by low
341 N concentration, and net MeHg production in response to leachate stimulus never increased to
342 vegetated levels. Importantly, leachate enhanced the relative abundance of putative methylators
343 within the microbiome in both environments, indicating that mercury methylation rates may be
344 dually influenced by the sediment microbiome and by organic matter[7,62].
345
346 *Microbiome response to leachate addition.*
347 Our results bolster support for recent work demonstrating preferential organic
348 degradation by *Clostridial* fermentation over oxidation by *Deltaproteobacteria*[63] and provide
349 support for the involvement of this clade in MeHg production. Within both environments,
350 leachate altered the sediment microbiome, with structural shifts denoting an increase in
351 *Clostridia* and decrease in *Deltaproteobacteria*. Unvegetated microcosms displayed greater
352 changes in these clades, supporting a greater role for environmental filtering by DOM within
353 oligotrophic environments[64,65]. *Clostridia* are obligate anaerobes with the ability to produce
354 labile carbon compounds via fermentation of recalcitrant organic matter[63,66]. Recent work has
355 shown organic carbon degradation via *Clostridial* fermentation to operate at comparable rates to
356 more energetically favorable carbon processing pathways[62]. Moreover, organic acids (*e.g.*,
357 lactate and acetate) produced through these pathways can be subsequently utilized as a carbon
358 source by sulfate- and iron- reducing *Deltaproteobacteria*[63,67,68]. Importantly, microbiome
359 changes were mirrored when examining putative methylators independently. Specifically,

360 *Deltaproteobacteria* and *Clostridia*, respectively, were the most abundant methylating organisms
361 at the end of the incubation in all experimental groups except no leachate vegetated microcosms.
362 In unvegetated sediments, although no methylating pathways were identified,
363 metagenomic analyses indicated an increase in carbon, and secondarily, iron metabolisms,
364 supporting a role for microbial carbon and iron cycling in mercury methylation[12,14,27,28]. Carbon
365 metabolisms were the primary KEGG category increasing in abundance within metagenomes
366 (Figure 3A), and several COG pathways and Pfams indicated a possible metabolic shift favoring
367 glycosyltransferases that convert starches, sugars, and nitroaromatics into a wide range of
368 compounds[69,70] (Figure 3B and C). Further, metagenomic increases in Beta-galactosidase/beta-
369 glucoronidase (lactose to galactose/glucose)[71], sugar phosphate isomerase/epimerases (sugar
370 metabolism)[72], and lactoylglutathione lyase (detoxification for methyglyoxal fermentation
371 byproduct)[73] and the SusD family (glycan binding)[74] provide additional evidence increases in
372 fermentation processes in response to leachate. Increases in TonB dependent receptors[75],
373 amidohydrolase[76], and NRAMP[77] suggest a secondary importance of iron processing and/or
374 transport of large organic compounds across cellular membranes. Finally, our results provide a
375 possible genetic mechanism connecting iron, sulfur, carbon, and mercury cycling, as the radical
376 SAM superfamily, which facilitates methyl transfers via the use of a [4Fe-S]+ cluster[78],
377 increased in concert with net MeHg production. In total, the metabolic potential of the sediment
378 microbiome indicates changes in carbon and iron metabolisms within microcosms experiencing
379 higher net MeHg production in response to leachate, supporting past work that suggests a linkage
380 between mercury methylation and these factors[7,12,14,27,28].
381 Lastly, at high taxonomic resolution in both environments, leachate increased the
382 proportion of methylating organisms classified as *Peptococcaceae* within *Clostridia*, despite

383 drastic differences in sediment chemistry (Figure 2D). Specifically, the two OTUs displaying the
384 greatest change are thought to generate energy via organohalide respiration (*D. restrictus*) and
385 fermentative oxidation of organic matter (*S. glycolicus*, also capable of syntrophy)[79,80]. The
386 relative abundance of *Peptococcaceae* was positively correlated with MeHg production in the
387 unvegetated environment, and other methylating organisms did not increase in abundance, as
388 would be expected if the activity of these organisms was enhanced by leachate.
389
390 *Associations between microbiology, DOM processing, and net MeHg production.*
391 The processing of proportionally more labile (microbe-preferred) organic matter would
392 be expected to result in decreases in DOM freshness and increases in HIX. However, our results
393 suggest substantial contributions of recalcitrant organic matter processing within the unvegetated
394 environment (but not the vegetated environment which followed expectations). In unvegetated
395 microcosms (both leachate and no leachate), HIX did not rise through time indicating relcatritant
396 matter processing (Figure 4C and D). Further, leachate unvegetated microcosms, which
397 experienced pronounced changes in the sediment microbiome and high MeHg production, HIX
398 was significantly lower than in all other experimental groups (ANOVA, $P < 0.0001$, all Tukey
399 HSD $P < 0.0001$). While most microorganisms preferentially degrade labile C sources, the
400 degradation of recalcitrant organic matter can contribute substantially to aquatic carbon
401 cycling[81]. Leachate unvegetated microcosms also exhibited large increases in microbially-
402 derived DOM (FI) through time, demonstrating a noticeable contribution of microbial activity to
403 the DOM pool (Figure 4A).
404 The abundance of methylating *Peptococcaceae* in unvegetated microcosms negatively
405 correlated with HIX, denoting an apparent contribution of these members or co-occuring

community members to DOM processing, but the mechanisms behind these shifts remain unclear. Metabolism of recalcitrant organic matter by fermenting organisms may influence mercury methylation via direct and indirect mechanisms. Members of *Clostridia* can generate MeHg themselves, and *Clostridial* degradation of recalcitrant organic matter can also produce bioavailable carbon substrates for sulfate- and iron- reducing organisms that produce MeHg[63].

Changes in metagenomes in responses to leachate elucidate metabolic pathways that may be involved in recalcitrant organic matter processing and MeHg production. For example, both COG and Pfam glycosyltransferases were negatively correlated with HIX, suggesting a role for starch, sugar, and nitroaromatic fermentation in response to DOM loading. As well, a negative correlation between HIX, and the radical SAM superfamily provides a possible mechanistic linkage between methyl transfers and recalcitrant organic matter processing. Conversely, Beta-galactosidase/beta-glucuronidase, and the SusD family were positively correlated with HIX, indicating a co-association with labile C processing rather than recalcitrant organic matter. Only one abundant Pfam – a TonB dependent receptor, signaling enzyme that may be involved in iron cycling[75] – and no COGs was correlated with MeHg production. Although our results do not provide a direct linkage between metabolic pathways and mercury methylation, it is notable that no pathways associations involve sulfate-reducing or methanogenic methylators.

Conclusions.

Microbiome shifts towards fermentation pathways, increases in chemoorganotrophic *Clostridia*, degradation of recalcitrant organic matter, and increases in MeHg within oligotrophic environments begin to elucidate the microbial ecology of mercury methylation. While we observed evidence for changes in the microbiome of both high-C and nutrient-poor sediment, the

more oligotrophic environment showed greater responses in the sediment microbiome and in mercury methylation to the addition of DOM, an important insight given increasing risks of anthropogenic eutrophication. Importantly, our results provide evidence for organisms not historically considered in MeHg production and suggest future work into the environmental relevance of these organisms in mercury methylation. *Clostridia* thrive in a variety of anoxic environments from wastewater effluent[82] to the human gut[83], and our work supports the potential for mercury methylation across a broad range of ecological niches[12,14]. Taken together, our research provides new insights into microorganisms impacting MeHg production in natural settings and emphasizes the importance of exploring microbial physiology not typically associated with methylating organisms in enhancing mercury toxicity.

Acknowledgements.

This work was supported by EPA STAR and NOAA NERRS fellowships to EBG and a JGI CSP grant to DRN. We also acknowledge support from the US Department of Energy (DOE), Office of Biological and Environmental Research (BER), as part of Subsurface Biogeochemical Research Program's Scientific Focus Area (SFA) at the Pacific Northwest National Laboratory (PNNL). PNNL is operated for DOE by Battelle under contract DE-AC06-76RLO 1830. We thank Alan Townsend, Teresa Bilinski, Deb Repert, Dick Smith, Steve Schmidt, Sharon Collinge, Garrett Rue, Jess Ebert, Alexis Templeton, and the LSNERR staff for valuable support and feedback during this project. We also thank Axios Review Service for valuable feedback on this manuscript.

Conflict of Interest.

452 The authors declare no conflict of interest.

453

454

455 **References.**

456 1 Benoit, J., Gilmour, C., Heyes, A., Mason, R. & Miller, C. Geochemical and biological
457 controls over methylmercury production and degradation in aquatic ecosystems. *ACS*
458 *symposium series* **835**, 262-297 (2003).
459 2 Ullrich, S. M., Tanton, T. W. & Abdrashitova, S. A. Mercury in the aquatic environment:
460 a review of factors affecting methylation. *Critical reviews in environmental science and*
461 *technology* **31**, 241-293 (2001).
462 3 Morel, F. M., Kraepiel, A. M. & Amyot, M. The chemical cycle and bioaccumulation of
463 mercury. *Annual review of ecology and systematics*, 543-566 (1998).
464 4 Harmon, S., King, J., Gladden, J., Chandler, G. T. & Newman, L. Mercury body burdens
465 in Gambusia holbrooki and Erimyzon sucetta in a wetland mesocosm amended with
466 sulfate. *Chemosphere* **59**, 227-233 (2005).
467 5 Branfireun, B. A., Roulet, N. T., Kelly, C. & Rudd, J. W. In situ sulphate stimulation of
468 mercury methylation in a boreal peatland: Toward a link between acid rain and
469 methylmercury contamination in remote environments. *Global Biogeochemical Cycles*
470 **13**, 743-750 (1999).
471 6 Jeremiason, J. D. *et al.* Sulfate addition increases methylmercury production in an
472 experimental wetland. *Environmental science & technology* **40**, 3800-3806 (2006).
473 7 Hsu-Kim, H., Kucharzyk, K. H., Zhang, T. & Deshusses, M. A. Mechanisms regulating
474 mercury bioavailability for methylating microorganisms in the aquatic environment: a
475 critical review. *Environmental science & technology* **47**, 2441-2456 (2013).
476 8 Ravichandran, M. Interactions between mercury and dissolved organic matter—a review.
477 *Chemosphere* **55**, 319-331 (2004).
478 9 Graham, A. M., Aiken, G. R. & Gilmour, C. C. Effect of dissolved organic matter source
479 and character on microbial Hg methylation in Hg–S–DOM solutions. *Environmental*
480 *science & technology* **47**, 5746-5754 (2013).
481 10 Parks, J. M. *et al.* The genetic basis for bacterial mercury methylation. *Science* **339**,
482 1332-1335 (2013).
483 11 Poulain, A. J. & Barkay, T. Cracking the mercury methylation code. *Science* **339**, 1280-
484 1281 (2013).
485 12 Gilmour, C. C. *et al.* Mercury methylation by novel microorganisms from new
486 environments. *Environmental science & technology* **47**, 11810-11820 (2013).
487 13 Smith, S. D. *et al.* Site-directed mutagenesis of HgcA and HgcB reveals amino acid
488 residues important for mercury methylation. *Applied and environmental microbiology* **81**,
489 3205-3217 (2015).
490 14 Podar, M. *et al.* Global prevalence and distribution of genes and microorganisms
491 involved in mercury methylation. *Science advances* **1**, e1500675 (2015).
492 15 Lambertsson, L. & Nilsson, M. Organic material: the primary control on mercury
493 methylation and ambient methyl mercury concentrations in estuarine sediments.
494 *Environmental science & technology* **40**, 1822-1829 (2006).
495 16 Wetzel, R. G. in *Dissolved organic matter in lacustrine ecosystems* 181-198 (Springer,
496 1992).
497 17 Haitzer, M., Aiken, G. R. & Ryan, J. N. Binding of mercury (II) to dissolved organic
498 matter: the role of the mercury-to-DOM concentration ratio. *Environmental Science &*
499 *Technology* **36**, 3564-3570 (2002).

18 Drexel, R. T., Haitzer, M., Ryan, J. N., Aiken, G. R. & Nagy, K. L. Mercury (II) sorption to two Florida Everglades peats: Evidence for strong and weak binding and competition by dissolved organic matter released from the peat. *Environmental science & technology* **36**, 4058-4064 (2002).

19 Waples, J. S., Nagy, K. L., Aiken, G. R. & Ryan, J. N. Dissolution of cinnabar (HgS) in the presence of natural organic matter. *Geochimica et Cosmochimica Acta* **69**, 1575-1588 (2005).

20 King, J. K., Kostka, J. E., Frischer, M. E. & Saunders, F. M. Sulfate-reducing bacteria methylate mercury at variable rates in pure culture and in marine sediments. *Applied and Environmental Microbiology* **66**, 2430-2437 (2000).

21 Docherty, K. M., Young, K. C., Maurice, P. A. & Bridgham, S. D. Dissolved organic matter concentration and quality influences upon structure and function of freshwater microbial communities. *Microbial Ecology* **52**, 378-388 (2006).

22 Pernthaler, J. in *The Prokaryotes* 97-112 (Springer, 2013).

23 Forsström, L., Roiha, T. & Rautio, M. Responses of microbial food web to increased allochthonous DOM in an oligotrophic subarctic lake. *Aquatic microbial ecology* **68**, 171-184 (2013).

24 Graham, E. B. *et al.* Microbes as engines of ecosystem function: When does community structure enhance predictions of ecosystem processes? *Frontiers in microbiology* **7** (2016).

25 Fellman, J. B., Hood, E. & Spencer, R. G. Fluorescence spectroscopy opens new windows into dissolved organic matter dynamics in freshwater ecosystems: A review. *Limnology and Oceanography* **55**, 2452-2462 (2010).

26 Compeau, G. & Bartha, R. Sulfate-reducing bacteria: principal methylators of mercury in anoxic estuarine sediment. *Applied and environmental microbiology* **50**, 498-502 (1985).

27 Kerin, E. J. *et al.* Mercury methylation by dissimilatory iron-reducing bacteria. *Applied and environmental microbiology* **72**, 7919-7921 (2006).

28 Hamelin, S., Amyot, M., Barkay, T., Wang, Y. & Planas, D. Methanogens: principal methylators of mercury in lake periphyton. *Environmental science & technology* **45**, 7693-7700 (2011).

29 Bae, H.-S., Dierberg, F. E. & Ogram, A. Syntrophs Dominate Sequences Associated with the Mercury Methylation-Related Gene hgcA in the Water Conservation Areas of the Florida Everglades. *Applied and environmental microbiology* **80**, 6517-6526 (2014).

30 Liu, Y.-R., Yu, R.-Q., Zheng, Y.-M. & He, J.-Z. Analysis of the Microbial Community Structure by Monitoring an Hg Methylation Gene (hgcA) in Paddy Soils along an Hg Gradient. *Applied and environmental microbiology* **80**, 2874-2879 (2014).

31 Hamelin, S., Planas, D. & Amyot, M. Mercury methylation and demethylation by periphyton biofilms and their host in a fluvial wetland of the St. Lawrence River (QC, Canada). *Science of the Total Environment* **512**, 464-471 (2015).

32 Liu, Y.-R., Zheng, Y.-M., Zhang, L.-M. & He, J.-Z. Linkage between community diversity of sulfate-reducing microorganisms and methylmercury concentration in paddy soil. *Environmental Science and Pollution Research* **21**, 1339-1348 (2014).

33 Lu, X. *et al.* Anaerobic mercury methylation and demethylation by Geobacter bemidjiensis Bem. *Environmental science & technology* **50**, 4366-4373 (2016).

34 Si, Y., Zou, Y., Liu, X., Si, X. & Mao, J. Mercury methylation coupled to iron reduction by dissimilatory iron-reducing bacteria. *Chemosphere* **122**, 206-212 (2015).

35 Yu, R.-Q., Reinfelder, J. R., Hines, M. E. & Barkay, T. Mercury methylation by the methanogen Methanospirillum hungatei. *Applied and environmental microbiology* **79**, 6325-6330 (2013).

36 Hintelmann, H., Keppel‐Jones, K. & Evans, R. D. Constants of mercury methylation and demethylation rates in sediments and comparison of tracer and ambient mercury availability. *Environmental toxicology and chemistry* **19**, 2204-2211 (2000).

37 Regnier, P. *et al.* Anthropogenic perturbation of the carbon fluxes from land to ocean. *Nature geoscience* **6**, 597-607 (2013).

38 Compeau, G. & Bartha, R. Methylation and demethylation of mercury under controlled redox, pH and salinity conditions. *Applied and Environmental Microbiology* **48**, 1203-1207 (1984).

39 Poulain, A. J. *et al.* Relationship between the loading rate of inorganic mercury to aquatic ecosystems and dissolved gaseous mercury production and evasion. *Chemosphere* **65**, 2199-2207 (2006).

40 Harris-Hellal, J., Vallaeys, T., Garnier-Zarli, E. & Bousserrhine, N. Effects of mercury on soil microbial communities in tropical soils of French Guyana. *Applied Soil Ecology* **41**, 59-68 (2009).

41 Zhou, Z. *et al.* Responses of activities, abundances and community structures of soil denitrifiers to short-term mercury stress. *Journal of Environmental Sciences* **24**, 369-375 (2012).

42 Ruggiero, P. *et al.* Hg bioavailability and impact on bacterial communities in a long-term polluted soil. *Journal of Environmental Monitoring* **13**, 145-156 (2011).

43 Gabor, R. S., Baker, A., McKnight, D. M. & Miller, M. P. Fluorescence Indices and Their Interpretation. *Aquatic Organic Matter Fluorescence*, 303 (2014).

44 Gabor, R. S., Eilers, K., McKnight, D. M., Fierer, N. & Anderson, S. P. From the litter layer to the saprolite: Chemical changes in water-soluble soil organic matter and their correlation to microbial community composition. *Soil Biology and Biochemistry* **68**, 166-176 (2014).

45 Knelman, J. E. *et al.* Bacterial community structure and function change in association with colonizer plants during early primary succession in a glacier forefield. *Soil Biology and Biochemistry* **46**, 172-180 (2012).

46 Caporaso, J. G. *et al.* Ultra-high-throughput microbial community analysis on the Illumina HiSeq and MiSeq platforms. *The ISME journal* **6**, 1621-1624 (2012).

47 Edgar, R. C. UPARSE: highly accurate OTU sequences from microbial amplicon reads. *Nature methods* **10**, 996-998 (2013).

48 Caporaso, J. G. *et al.* QIIME allows analysis of high-throughput community sequencing data. *Nature methods* **7**, 335-336 (2010).

49 Finn, R. D. Pfam: the protein families database. *Encyclopedia of Genetics, Genomics, Proteomics and Bioinformatics* (2012).

50 Tatusov, R. L. *et al.* The COG database: an updated version includes eukaryotes. *BMC bioinformatics* **4**, 1 (2003).

51 Kanehisa, M. & Goto, S. KEGG: kyoto encyclopedia of genes and genomes. *Nucleic acids research* **28**, 27-30 (2000).

52 Markowitz, V. M. *et al.* IMG: the integrated microbial genomes database and comparative analysis system. *Nucleic acids research* **40**, D115-D122 (2012).

53 Benson, D. A. *et al.* GenBank. *Nucleic acids research* **41**, D36-D42 (2013).

592 54 Lozupone, C., Lladser, M. E., Knights, D., Stombaugh, J. & Knight, R. UniFrac: an
593 effective distance metric for microbial community comparison. *The ISME journal* **5**, 169
594 (2011).
595 55 Taylor, P. G. & Townsend, A. R. Stoichiometric control of organic carbon–nitrate
596 relationships from soils to the sea. *Nature* **464**, 1178-1181 (2010).
597 56 Windham‐Myers, L. *et al.* Experimental removal of wetland emergent vegetation leads
598 to decreased methylmercury production in surface sediment. *Journal of Geophysical*
599 *Research: Biogeosciences (2005–2012)* **114** (2009).
600 57 Roy, V., Amyot, M. & Carignan, R. Beaver ponds increase methylmercury
601 concentrations in Canadian shield streams along vegetation and pond-age gradients.
602 *Environmental science & technology* **43**, 5605-5611 (2009).
603 58 Windham-Myers, L. *et al.* Mercury cycling in agricultural and managed wetlands of
604 California, USA: Experimental evidence of vegetation-driven changes in sediment
605 biogeochemistry and methylmercury production. *Science of the Total Environment* **484**,
606 300-307 (2014).
607 59 Wett, B. & Rauch, W. The role of inorganic carbon limitation in biological nitrogen
608 removal of extremely ammonia concentrated wastewater. *Water Research* **37**, 1100-1110
609 (2003).
610 60 Bradley, P., Fernandez Jr, M. & Chapelle, F. Carbon limitation of denitrification rates in
611 an anaerobic groundwater system. *Environmental science & technology* **26**, 2377-2381
612 (1992).
613 61 Brooks, P. D., McKnight, D. & Elder, K. Carbon limitation of soil respiration under
614 winter snowpacks: potential feedbacks between growing season and winter carbon fluxes.
615 *Global Change Biology* **11**, 231-238 (2005).
616 62 Aiken, G. R., Hsu-Kim, H. & Ryan, J. N. Influence of dissolved organic matter on the
617 environmental fate of metals, nanoparticles, and colloids. *Environmental science &*
618 *technology* **45**, 3196-3201 (2011).
619 63 Reimers, C. E. *et al.* Redox effects on the microbial degradation of refractory organic
620 matter in marine sediments. *Geochimica et Cosmochimica Acta* **121**, 582-598 (2013).
621 64 Stegen, J. C., Lin, X., Konopka, A. E. & Fredrickson, J. K. Stochastic and deterministic
622 assembly processes in subsurface microbial communities. *The ISME journal* **6**, 1653-
623 1664 (2012).
624 65 Barberán, A., Bates, S. T., Casamayor, E. O. & Fierer, N. Using network analysis to
625 explore co-occurrence patterns in soil microbial communities. *The ISME journal* **6**, 343-
626 351 (2012).
627 66 Ueno, A. *et al.* Anaerobic decomposition of humic substances by Clostridium from the
628 deep subsurface. *Scientific reports* **6** (2016).
629 67 Zhao, Y., Ren, N. & Wang, A. Contributions of fermentative acidogenic bacteria and
630 sulfate-reducing bacteria to lactate degradation and sulfate reduction. *Chemosphere* **72**,
631 233-242 (2008).
632 68 Guerrero-Barajas, C., Garibay-Orijel, C. & Rosas-Rocha, L. E. Sulfate reduction and
633 trichloroethylene biodegradation by a marine microbial community from hydrothermal
634 vents sediments. *International Biodeterioration & Biodegradation* **65**, 116-123 (2011).
635 69 Bowles, D., Isayenkova, J., Lim, E.-K. & Poppenberger, B. Glycosyltransferases:
636 managers of small molecules. *Current opinion in plant biology* **8**, 254-263 (2005).

637 70 Ramli, N., Abd-Aziz, S., Hassan, M. A., Alitheen, N. & Kamaruddin, K. Potential
638 cyclodextrin glycosyltransferase producer from locally isolated bacteria. *African Journal*
639 *of Biotechnology* **9**, 7317-7321 (2015).
640 71 Martini, M. C., Bollweg, G. L., Levitt, M. D. & Savaiano, D. A. Lactose digestion by
641 yogurt beta-galactosidase: influence of pH and microbial cell integrity. *The American*
642 *journal of clinical nutrition* **45**, 432-436 (1987).
643 72 Yeom, S.-J., Kim, Y.-S. & Oh, D.-K. Development of Novel Sugar Isomerases by
644 Optimization of Active Sites in Phosphosugar Isomerases for Monosaccharides. *Applied*
645 *and environmental microbiology* **79**, 982-988 (2013).
646 73 Inoue, Y. & Kimura, A. Methylglyoxal and regulation of its metabolism in
647 microorganisms. *Advances in microbial physiology* **37**, 177 (1995).
648 74 Martens, E. C., Koropatkin, N. M., Smith, T. J. & Gordon, J. I. Complex glycan
649 catabolism by the human gut microbiota: the Bacteroidetes Sus-like paradigm. *Journal of*
650 *Biological Chemistry* **284**, 24673-24677 (2009).
651 75 Moeck, G. S. & Coulton, J. W. TonB‐dependent iron acquisition: Mechanisms of
652 siderophore‐mediated active transport. *Molecular microbiology* **28**, 675-681 (1998).
653 76 Seibert, C. M. & Raushel, F. M. Structural and catalytic diversity within the
654 amidohydrolase superfamily. *Biochemistry* **44**, 6383-6391 (2005).
655 77 Cellier, M. *et al.* Nramp defines a family of membrane proteins. *Proceedings of the*
656 *National Academy of Sciences* **92**, 10089-10093 (1995).
657 78 Booker, S. J. & Grove, T. L. Mechanistic and functional versatility of radical SAM
658 enzymes. *F1000 Biol. Rep* **2**, 52 (2010).
659 79 Stackebrandt, E. in *The Prokaryotes* 285-290 (Springer, 2014).
660 80 Han, C. *et al.* Complete genome sequence of Syntrophobotulus glycolicus type strain
661 (FlGlyRT). *Standards in genomic sciences* **4**, 371 (2011).
662 81 Mcleod, E. *et al.* A blueprint for blue carbon: toward an improved understanding of the
663 role of vegetated coastal habitats in sequestering CO2. *Frontiers in Ecology and the*
664 *Environment* **9**, 552-560 (2011).
665 82 Wang, C. *et al.* Producing hydrogen from wastewater sludge by Clostridium
666 bifermentans. *Journal of Biotechnology* **102**, 83-92 (2003).
667 83 Mahowald, M. A. *et al.* Characterizing a model human gut microbiota composed of
668 members of its two dominant bacterial phyla. *Proceedings of the National Academy of*
669 *Sciences* **106**, 5859-5864 (2009).

670

671

672 **Figures.**

Figure 1

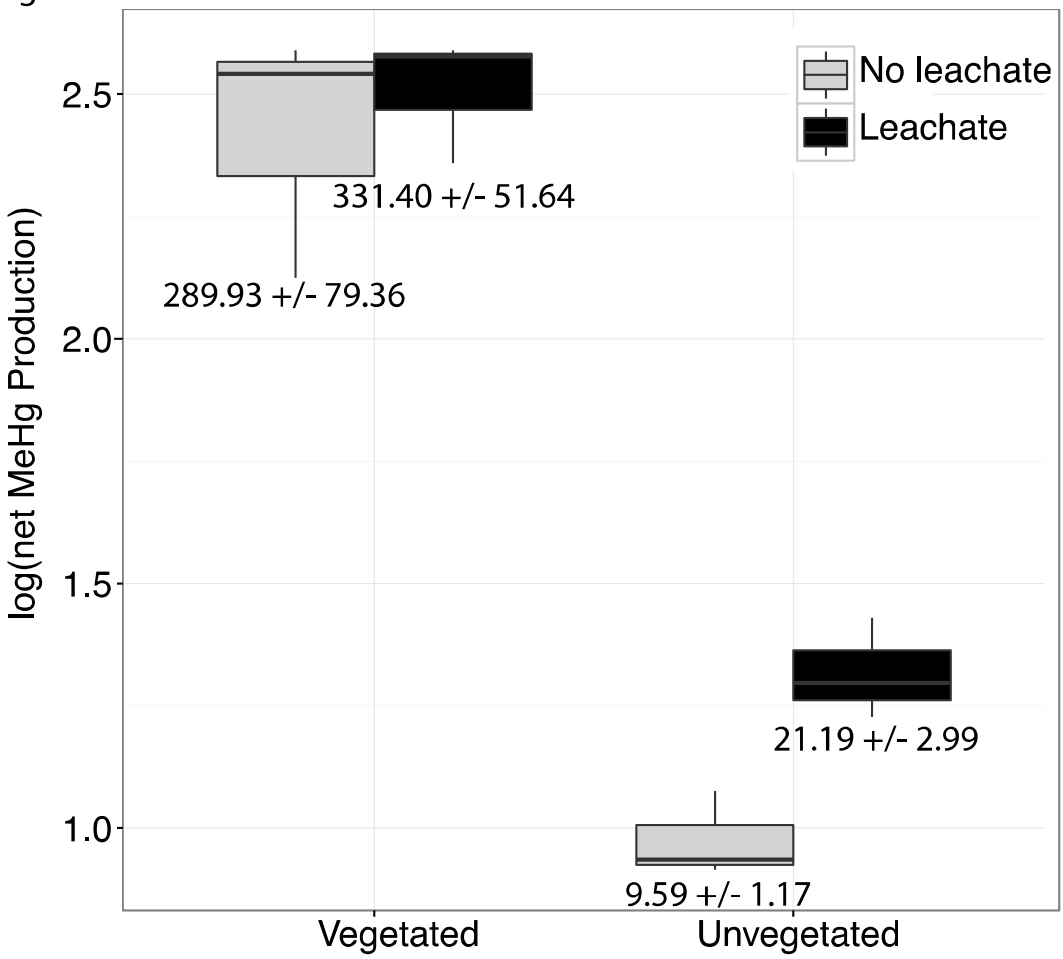

673

674 **Figure 1.** Boxplots are shown for net MeHg production (calculated as concentration at 28 days
675 less the initial concentration), with upper and lower hinges representing the values at the 75th and
676 25th percentiles and whiskers representing 1.5 times value at the 75th and 25th percentiles,
677 respectively. Leachate increased net MeHg production in unvegetated sediment but did not have
678 a large impact within vegetated sediments. Regardless of leachate addition, vegetated sediment
679 experienced an order of magnitude higher rates of net mercury methylation. Mean increase in
680 MeHg production in ng per g dry +/- standard errors are listed below each box.

681

Figure 2

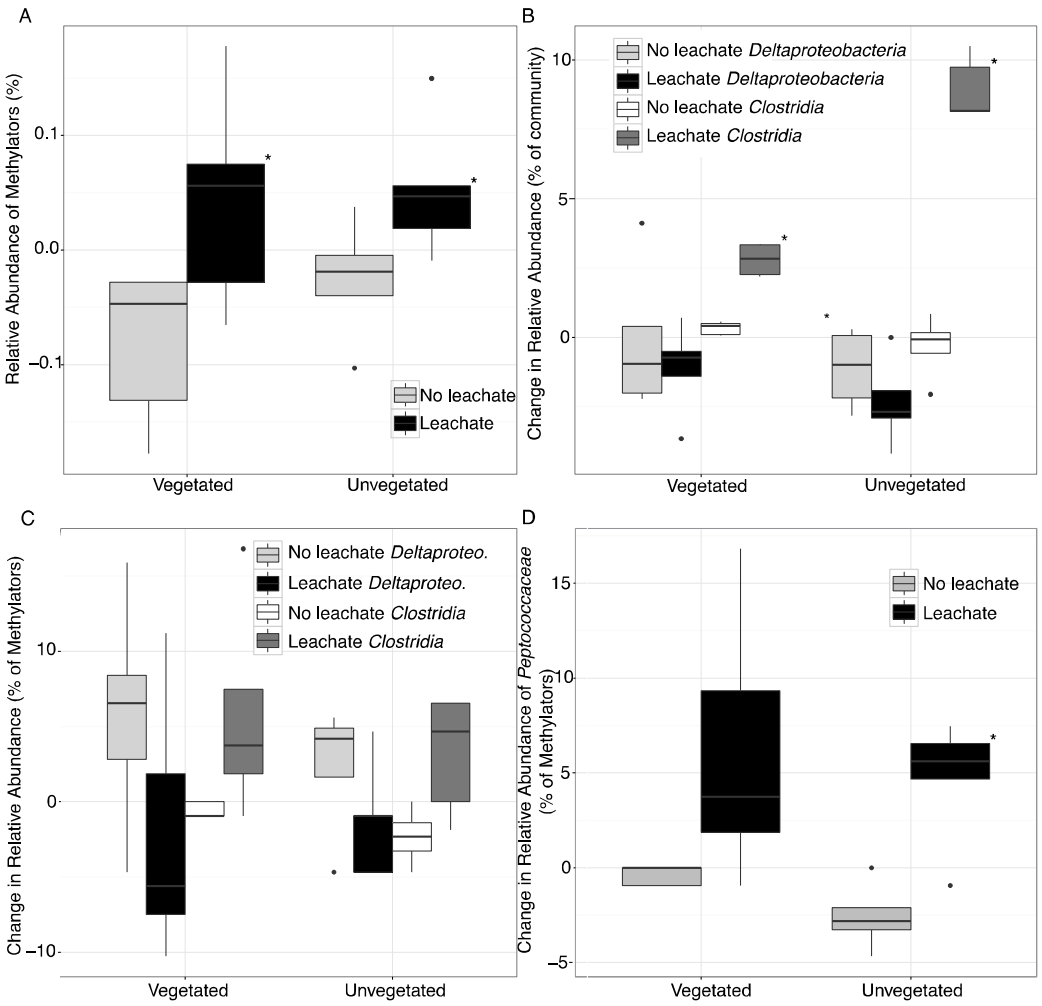

682

683 **Figure 2.** Boxplots are shown for selected changes in abundance of methylator abundance (A)
684 and taxonomy (B-D) in response to leachate addition, with upper and lower hinges representing
685 the values at the 75th and 25th percentiles and whiskers representing 1.5 times value at the 75th
686 and 25th percentiles, respectively. Outliers are plotted as points. Shading for each bar denote
687 taxonomy and leachate vs. no leachate. Significant relationships ($P < 0.05$) are denoted with an
688 asterisk. (A) The relative abundance of methylating organisms increased in both sediment types
689 in response to leachate addition. (B) The addition of leachate decreased the proportion of

690 *Deltaproteobacteria* and increased the proportion of *Clostridia* in both vegetated and
691 unvegetated sediment, with greater effects in unvegetated sediment. (C) Within potential
692 methylators, *Deltaproteobacteria* decreased and *Clostridia* increased in response to leachate, (D)
693 driven by changes within the family *Peptococcaceae*. Abundance data are present in Table S3.
694
695

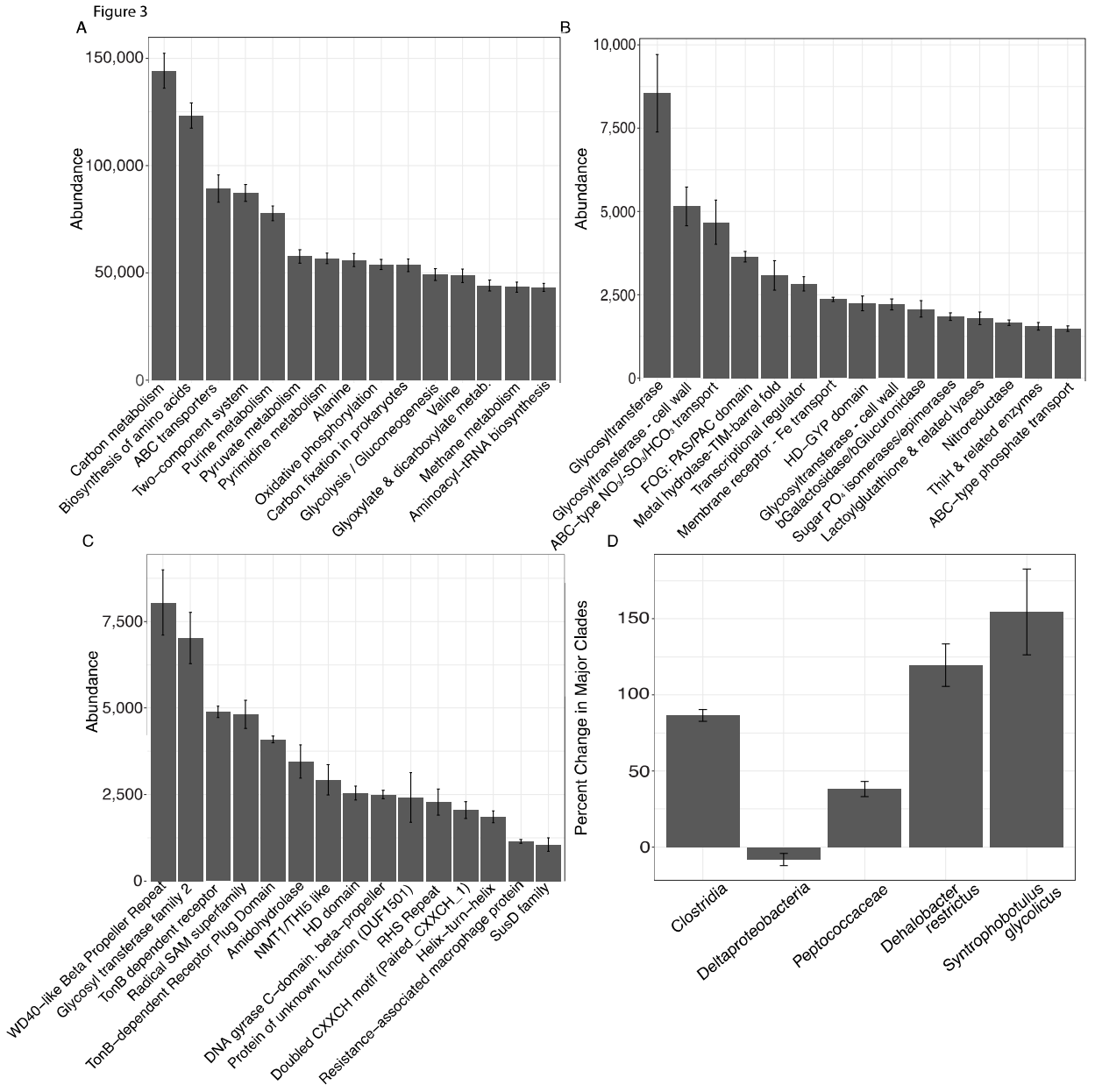

Figure 3. Results from analysis of metagenomic shotgun sequences from unvegetated microcosms are denoted in Figure 3. Panels A, B, and C show the abundance of the top 15 KEGG, COG, and Pfam targets that increased at day 28 vs. day 0, respectively. Panel D shows percent change in selected taxonomic groups at day 28 vs. day 0. Error bars denote standard error.

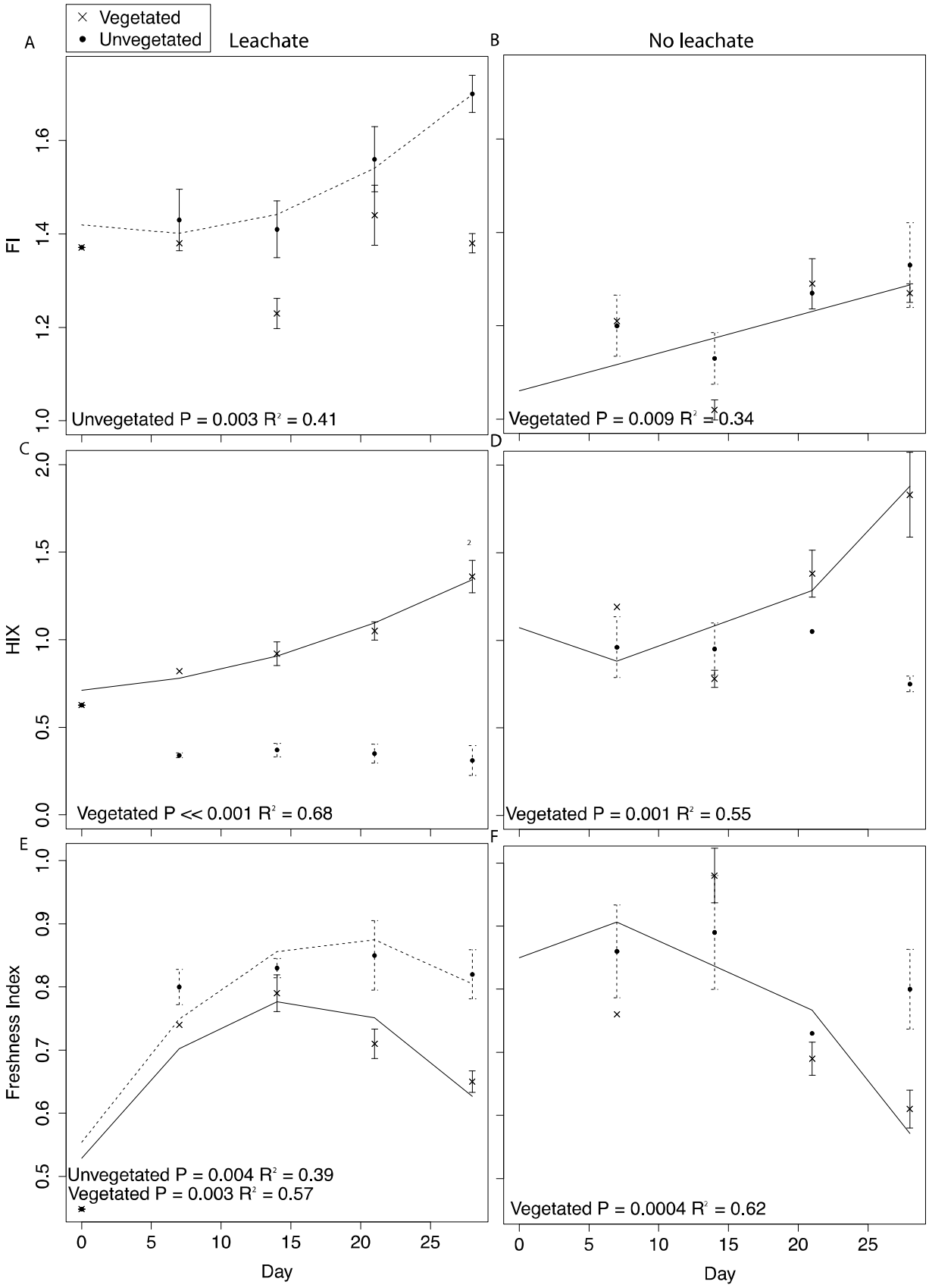

703

Figure 4. DOM fluorescence indices were assessed through time with linear and quadratic regressions in each environment and microcosm type. Averages for each environment and microcosm type are plotted at days 0, 7, 14, 21, and 28, with error bars representing the standard error. Plots in the first column are leachate microcosms, while plots in the second column are no leachate microcosms. Unvegetated microcosms are depicted as closed circles with dashed lines showing significant regressions; vegetated microcosms are x's with solid lines showing significant regressions. (A) and (B) denote FI, (C) and (D) denote HIX, and (E) and (F) denote freshness.

714 **Tables.**

715

716 **Table 1.** Mean chemical and biological characteristics of vegetated (*n* = 5) and unvegetated (n =
717 5) environments are presented Table 1. Asterisks represent significant differences from post hoc
718 *t*-tests, and standard deviations are presented in parentheses.

	Vegetated Environment	Unvegetated Environment
pH*	5.6 (0.09)	5.8 (0.40)
NH4 (mg/L)***	1.49 (0.32)	0.36 (0.14)
TPOC (mg/L)***	1.13 (0.06)	0.09 (0.05)
TDN (mg/L)**	0.06 (0.02)	0.04 (0.01)
percent C***	13.16 (2.20)	1.82 (3.39)
percent N***	0.8 (0.06)	0.1 (0.23)
C:N*	16.43 (1.59)	20.06 (5.36)
DNA concentratin (ng/L)***	28.13 (5.06)	9.31 (3.16)
NAG (nmol/h/g)***	308.94 (81.30)	9.05 (9.29)
BG (nmol/h/g)***	371.22 (81.25)	17.71 (19.29)
PHOS (nmol/h/g)***	393.45 (55.06)	20.69 (17.33)
SMHG (ng/g)**	2.67 (2.18)	0.24 (0.12)
STHG (ng/g)	306.56 (551.07)	3.16 (3.99)
SM/THG	0.02 (0.009)	0.32 (0.45)
Proteobacteria***	0.3 (0.04)	0.43 (0.02)
Chloroflexi***	0.17 (0.01)	0.06 (0.009)
Bacteroidetes	0.11 (0.02)	0.13 (0.03)
Acidobacteria*	0.07 (0.009)	0.08 (0.02)
Nitrospirae***	0.05 (0.009)	0.02 (0.009)
Actinobacteria***	0.03 (0.007)	0.07 (0.01)
Alpha Diversity**	183.8 (6.64)	193.7 (11.33)

*$P \leq 0.10$ **$P \leq 0.05$ ***$P \leq 0.01$

719
720

722

723 **Table 2.** R^2 values from regression analysis of changes in DOM properties through time are listed in Table 2. No leachate microcosms
724 were analyzed from across days 7, 14, 21, and 28; and leachate microcosms were analyzed across days 0, 7, 14, 21, and 28 (*n* = 4-5 at
725 each sampling point, no samples were taken in no leachate microcosms at day zero), with characteristics of the applied leachate
726 represented at day 0.

	NPOC (mg/L)	Total Fluoresence	Fluor:NPOC	FI	HIX	Freshness
Vegetated, No leachate (across days 7, 14, 21, 28)	0.39**	0.21*	n.s.	0.22**	0.51***	0.52***
Vegetated, Leachate (across days 0, 7, 14, 21, 28)	0.32***	n.s.	n.s.	n.s.	0.68****	0.57***
Unvegetated, No leachate across days 7, 14, 21, 28)	0.64****	n.s.	0.29**	n.s.	n.s.	n.s.
Unvegetated, Leachate (across days 0, 7, 14, 21, 28)	n.s.	n.s.	n.s.	0.41***	n.s.	0.39***

727 * $P < 0.10$ ** $P < 0.05$ *** $P < 0.01$ **** $P < 0.001$

728

729 **Table 3.** The Pearson product-momentum correlation coefficient was used to assess relationships of selected COG and Pfam targets
730 with HIX and net MeHg production at day 28 (n = 3). Relationships are presented in Table 3.

	HIX	MeHg
COG		
Glycosyltransferase	0.98*	0.79
Glycosyltransferases involved in cell wall biogenesis	0.96*	0.76
ABC-type nitrate/sulfonate/bicarbonate transport systems, periplasmic components	-0.85	0.55
FOG: PAS/PAC domain	-0.88	0.60
Predicted metal-dependent hydrolase of the TIM-barrel fold	0.88	0.60
Transcriptional regulator	0.999**	0.88
Outer membrane receptor proteins, mostly Fe transport	-0.79	0.45
HD-GYP domain	0.99**	0.84
Glycosyltransferases, probably involved in cell wall biogenesis	0.96*	0.74
Beta-galactosidase/beta-glucuronidase	0.98*	-0.80
Sugar phosphate isomerases/epimerases	-0.73	0.36
Lactoylglutathione lyase and related lyases	-0.93	0.67
Nitroreductase	0.996**	0.86
Thiamine biosynthesis enzyme, ThiH and related uncharacterized enzymes	0.98*	0.80
ABC-type phosphate transport system, periplasmic component	-0.66	0.27
Pfam		
WD40-like Beta Propeller Repeat	0.99**	0.85
Glycosyl transferase family 2	0.97*	0.76
TonB dependent receptor	0.90	0.9999***
Radical SAM superfamily	0.95*	0.75
TonB-dependent Receptor Plug Domain	0.51	-0.83
Amidohydrolase	-0.87	0.57
NMT1/THI5 like	-0.87	0.58
HD domain	0.9997**	0.91
DNA gyrase C-terminal domain, beta-propeller	-0.94	0.70
Protein of unknown function (DUF1501)	-0.46	0.04
RHS Repeat	-0.80	0.46
Doubled CXXCH motif (Paired_CXXCH_1)	0.97*	0.78
Helix-turn-helix	-0.90	0.63
Natural resistance-associated macrophage protein	-0.83	0.51
SusD family	0.99*	-0.82

* $P < 0.10$ ** $P < 0.05$